Biogeosciences Discuss., doi:10.5194/bg-2016-194, 2016
Manuscript under review for journal Biogeosciences
Published: 17 May 2016

Biogeosciences Discussions
Open Access
EGU

Seasonal and vertical variations in soil CO_2 production in a beech forest: an isotopic flux-gradient approach

Emilie Delogu[1], Bernard Longdoz[1], Caroline Plain[1] & Daniel Epron[1]

[1] Université de Lorraine, INRA centre de Nancy-Lorraine, UMR 1137, Ecologie et Ecophysiologie Forestières, Faculté des Sciences, F-54500 Vandoeuvre-les-Nancy, France

Correspondence to: Emilie Delogu (emilie.delogu@gmail.com)

Abstract. Soil CO_2 efflux results from the transport of CO_2 from several respiration sources within the soil profile. A flux – gradient approach (FGA) was used to assess the vertical profile of CO_2 production (P_CO_2) and its isotopic composition ($\delta^{13}P\_CO_2$) from the measurement of the vertical profile of CO_2 concentration and CO_2 isotopic composition combined with soil CO_2 and $\delta^{13}CO_2$ effluxes. Variations in P_CO_2 and $\delta^{13}P\_CO_2$ within different soil layers were analyzed at different time scales. In the first soil layers, P_CO_2 was probably underestimated and $\delta^{13}P\_CO_2$ overestimated when CO_2 transport was not solely diffusive. At the seasonal scale, a vertical gradient of P_CO_2 temperature sensitivity was observed. At the within-day scale, variations in soil temperature were too weak to explain the strong variations in P_CO_2. At the daily time scale, $\delta^{13}P\_CO_2$ of sources located between -10 and -20 cm depth was well correlated with the canopy inherent water use efficiency (IWUE) measured the day before. The strong correlation with IWUE argues in favor of an actual connection between canopy activity and soil autotrophic production. Moreover, including SWC of the current day as a second variable improved the linear regression between $\delta^{13}P\_CO_2$ and IWUE of the previous day, together explaining 76% of the daily fluctuations in $\delta^{13}P\_CO_2$. This highlights the actual contribution of both autotrophic and heterotrophic sources to soil P_CO_2. The method used gave consistent and promising results even if we could not disentangle the respective contribution of autotrophic and heterotrophic sources to CO_2 production as the differences in their isotopic composition were too small and fluctuated too much. In addition, CO_2 transport by turbulent advection and dispersion will need to be considered for the top soil layer.

Keywords. Soil CO_2 production, carbon isotopes, vertical partitioning, diffusion, seasonal variability.

Biogeosciences Discuss., doi:10.5194/bg-2016-194, 2016
Manuscript under review for journal Biogeosciences
Published: 17 May 2016

1. Introduction

Soil CO_2 efflux (F_S) is the major component of CO_2 emissions in terrestrial ecosystems (Ryan and Law, 2005) and represents 60% to 80% of the total respiration in forest ecosystems (Granier et al., 2000; Janssens et al., 2003; Law et al., 1999). Accurate evaluations of F_S and of its response to environmental factors are essential for predicting changes in the terrestrial carbon balance (Ryan and Law, 2005). To better characterize and model this flux, it is essential to understand the multiple complex processes contributing to F_S (Subke et al., 2006). Although several empirical models have been used to describe the response of F_S to soil temperature and soil water content, which are the main drivers accounting for its temporal variations at a seasonal scale (Davidson et al., 1998; Epron et al., 1999; Janssens and Pilegaard, 2003), further efforts are required to better understand the short-term dynamics of F_S (Goffin et al., 2014; Moyes et al., 2010; Vargas et al., 2011, 2012).

F_S is the result of CO_2 production (P_CO_2) in the soil through respiration of two main types of sources (autotrophic and heterotrophic) and of CO_2 transport up into the atmosphere (Fang and Moncrieff, 1999). The autotrophic sources include the respiration of roots and rhizospheric microorganisms while the heterotrophic sources are related to soil microorganisms decomposing soil organic matter (Epron, 2009; Subke et al., 2006). Both the autotrophic and heterotrophic components of the soil CO_2 efflux have their own responses to their multiple drivers (Boone et al., 1998; Epron et al., 2001; Suleau et al., 2011). In consequence, soil CO_2 efflux is dependent on soil temperature and moisture (Davidson et al., 1998), on soil porosity and tortuosity (Werner et al., 2004), on air pressure and turbulence fluctuations at the soil surface (Maier et al., 2012), on the quality and quantity of decomposable organic substrates (Conant et al., 2011) and on the soil microorganism community (Karhu et al., 2014). Moreover, several studies have shown evidence of a link between photosynthesis and soil CO_2 efflux (Kuzyakov and Gavrichkova, 2010; Risk et al., 2012; Wingate et al., 2010). Stable isotopes have become a useful tool in understanding the complexity of the processes involved in soil CO_2 efflux and in assessing the relative contributions of autotrophic and heterotrophic sources (Bowling et al., 2008; Marron et al., 2009; Prévost-Bouré et al., 2008). Variations in the C isotopic composition of F_S ($\delta^{13}F_S$) have been related to soil moisture, temperature, rain events or vapor pressure deficit (Bowling et al., 2002; Ekblad et al., 2004; Fessenden and Ehleringer, 2003; Wingate et al., 2010). The latter relationship is part of the link between $\delta^{13}F_S$ and stomatal conductance or photosynthesis (Ekblad and Högberg, 2001; Lai et al., 2005; Bowling et al., 2008).

Many of these studies consider that the CO_2 released by the soil surface corresponds to the amount of CO_2 produced simultaneously within the soil, and that $\delta^{13}Fs$ represents the actual isotopic signature of the mixture of all the CO_2 sources. However, CO_2 can be stored during its transport towards the soil surface, thus inducing differences between P and F_S. In addition, CO_2 transport is driven mainly by diffusion (Davidson et al., 2006b; Pumpanen et al., 2008) and some fluctuations in the fractionation rate can occur during this CO_2 diffusion (Cerling et al., 1991). This may induce differences between the isotopic composition of CO_2 production ($\delta^{13}P\_CO_2$) and $\delta^{13}F_S$ (Moyes et al., 2010). As a consequence, a more precise understanding of the processes underlying CO_2 efflux requires formally separating production and transport mechanisms within the vertical soil profile. As the main biotic (roots, microorganisms) and abiotic (soil temperature, soil water content,

Biogeosciences Discuss., doi:10.5194/bg-2016-194, 2016
Manuscript under review for journal Biogeosciences
Published: 17 May 2016

substrate quality and quantity) drivers influencing P_CO_2 present a strong vertical variability through the soil profile (Davidson et al., 2006b), the analysis of the vertical distribution of P_CO_2 sources is also essential to evaluate the vertical partitioning of the subsurface CO_2 processes (Davidson et al., 2006b; Goffin et al., 2014; Jassal et al., 2004; Pumpanen et al., 2003). However, vertical variability has seldom been taken into account.

The flux – gradient approach (FGA - Jong and Schappert, 1972) has already been used to assess the vertical profile of P_CO_2 and δ^{13}P_CO_2 from the measurement of the [CO_2] vertical profile and its isotopic composition, F_S and $\delta^{13}F_S$ (Goffin et al., 2014). All these variables can be recorded simultaneously (Parent et al., 2013), thus providing insights into the mechanisms affecting production and transport.

Our objectives were, first, to quantify the contribution of the different soil layers to CO_2 production and to its isotopic signature, and secondly, to examine the variability of these contributions at different time scales. We used the FGA approach to analyze and understand the constraints on vertical and seasonal variations in P_CO_2 and δ^{13}P_CO_2. We further related the seasonal variations to soil temperature and soil water content. We then investigated the impacts of canopy processes on daily variations in δ^{13}P_CO_2. The autotrophic signal was tracked up in soil CO_2 production P_CO_2, thanks to the isotope composition of trunk respiration, the gross primary production and the evapotranspiration measured by a nearby eddy flux tower.

2. Materials and methods

2.1. The flux – gradient approach

When the soil is considered as a one-dimensional structure (horizontal homogeneity), the CO_2 production (P_CO_2, µmol m^{-3} s^{-1}) at each depth (z, m) is derived from the corresponding one-dimensional mass balance equation for CO_2:

$$\frac{\partial(\varepsilon[CO_2])}{\partial t} = \frac{\partial F}{\partial z} + P\_CO_2 \quad [1]$$

where ε is the air-filled porosity (m^3 m^{-3}), [CO_2] is the CO_2 concentration by m^3 of soil (µmol m^{-3}), F is the CO_2 vertical flux (µmol m^{-2} s^{-1}), t is the time (s) and z is the depth (m) for which all the variables of Eq. 1 are considered.

We divided the soil profile into five-centimeter-thick sections. Each section was characterized by a set of physical parameters (effective soil diffusion coefficient, porosity) and by environmental conditions (soil water content SWC, soil temperature T, [CO_2]). In each section i, P_CO_2 was calculated using the discrete form of Eq. 1:

$$P\_CO_{2\ i} = \frac{\Delta(\varepsilon_i \times [CO_2]_i)}{\Delta t} + \frac{F_{top,i} - F_{bot,i}}{\Delta z} \quad [2]$$

where $\frac{\Delta(\varepsilon_i \times [CO_2]_i)}{\Delta t}$ is the storage flux (µmol m^{-3} s^{-1}), and F_{top} and F_{bot} (µmol m^{-2} s^{-1}) are the gas fluxes transported through the upper and lower limits of the section, respectively.

Because diffusion was the only transport mechanism considered (see discussion), the flux (F) is expressed by Fick's first law:

Biogeosciences Discuss., doi:10.5194/bg-2016-194, 2016
Manuscript under review for journal Biogeosciences
Published: 17 May 2016

$$F_{top,i} = -\overline{Ds_{i,i+1}} \frac{[CO_2]_{i+1} - [CO_2]_i}{\Delta z} \quad [3]$$

$$F_{bot,i} = -\overline{Ds_{i-1,i}} \frac{[CO_2]_i - [CO_2]_{i-1}}{\Delta z} \quad [4]$$

where Ds is the effective soil diffusion coefficient (m^2 s^{-1}), $\overline{Ds_{x,y}}$ corresponds to the harmonic mean value between the Ds of the x (Ds_x) and y (Ds_y) sections and Δz is the section thickness (m).

How we determined $[CO_2]_i$, Ds_i and ε_i is presented in the following sections.

Eq. 2-4 were applied successively to $^{12}CO_2$ and $^{13}CO_2$ with their respective concentration and soil diffusion coefficient (Ds^{12} and Ds^{13}) to determine the production of these two isotopologues ($^{12}P\_CO_2$ and $^{13}P\_CO_2$). For each section, total production (P_i) and its isotopic composition ($\delta^{13}P\_CO_{2\ i}$, expressed in ‰) were calculated as follows:

$$P\_CO_{2_i} = {}^{12}P\_CO_{2_i} + {}^{13}P\_CO_{2_i} \quad [5]$$

$$\delta^{13}P\_CO_{2_i} = \left(\frac{1}{R_{std}} \times \frac{{}^{13}P\_CO_{2_i}}{{}^{12}P\_CO_{2_i}} - 1 \right) \times 1000 \quad [6]$$

where R_{std} is the isotopic ratio of the V-PDB reference standard.

2.2. Site description

The experiment was conducted in the Hesse beech forest located in north-eastern France (48°40' N, 7°05' E). The mean annual temperature (1997-2014) is 10.3°C and the mean annual precipitation is 979 mm. The soil is a Stagnic Luvisol (FAO, 2006) with a pH of 4.9 and containing 10 kg of organic carbon per m². A more detailed description is given by Granier et al. (2000).

The five-centimeter- thick sections in the FGA were part of three distinct layers in the soil vertical profile: [1] 0 to -10 cm, [2] -10 cm to -20 cm and [3] -20 to -40 cm (Fig.1). The two first layers contained each one third of total root biomass according to the root vertical profile (Peiffer et al., 2005). The soil texture is silt loam with 22% of clay in the first 20 centimeters and 34% below.

2.3. Field measurements

2.3.1. Tree trunk CO_2 efflux (F_t), soil CO_2 efflux (F_s) and their isotopic signatures ($\delta^{13}F_t$ and $\delta^{13}F_s$)

We used steady-state flow-through chambers (Marron et al., 2009; Plain et al., 2009) with a tunable diode laser absorption spectrometer (TDLAS, TGA 100A, Campbell Scientific) to measure [$^{12}CO_2$] and [$^{13}CO_2$] concentrations at inlet and outlet, accounting for the fraction of all CO_2 isotopologues other than $^{12}C^{16}O^{16}O$ and $^{13}C^{16}O^{16}O$ (0.00474, (Griffis et al., 2004)). Soil CO_2 efflux (F_s), trunk CO_2 efflux (F_t) and their isotopic signatures ($\delta^{13}F_s$ and $\delta^{13}F_t$) were calculated according to the following equations:

Biogeosciences Discuss., doi:10.5194/bg-2016-194, 2016
Manuscript under review for journal Biogeosciences
Published: 17 May 2016

$$F_x = \frac{([CO_2]_{out} - [CO_2]_{in}) \times Pa \times \phi}{8.314 \times T \times S} \quad [7]$$

where F_x represents F_t or F_s (µmol m^{-2} s^{-1}), $[CO_2]_{in}$ and $[CO_2]_{out}$ represent the CO_2 concentrations (µmol mol^{-1}) at the inlet and outlet of the chamber respectively, Pa is the atmospheric pressure (Pa), ϕ is the airflow rate through the chamber (m^3 s^{-1}), S is the soil or trunk surface inside the chamber (m^2), T is the air temperature (K), and 8.314 J mol^{-1} K^{-1} is the ideal gas constant.

$$\delta^{13}F_x = \left[\frac{1}{R_{std}} \times \left(\frac{\left[^{13}CO_2\right]_{out} - \left[^{13}CO_2\right]_{in}}{\left[^{12}CO_2\right]_{out} - \left[^{12}CO_2\right]_{in}}\right) - 1\right] \times 1000 \quad [8]$$

where $\delta^{13}F_x$ represents $\delta^{13}F_t$ or $\delta^{13}F_s$ (‰).

Soil chambers were made of stainless steel and allowed the enclosure of 314 cm^2 of soil. The chambers were composed of a 12.5-cm-high collar covered with mobile lids. Six collars were installed and every week, two of the four lids were moved to free collars in order to prevent a permanent soil covering. Consequently, each week's data set is composed of measurements from different combinations of four collars. To achieve a homogeneous time series, a gap filling procedure was performed for each collar during the periods when no measurements were conducted on it. This procedure is based on linear regressions between the different collar measurements (Goffin et al., 2014). The time series for each collar was compared with the time series of all the other collars and the linear equation from the best regression was chosen for gap filling. Mean F_s and $\delta^{13}F_s$ were estimated as the average values of all the collars after gap filling.

F_t and $\delta^{13}F_t$ were measured using two trunk chambers set up at the base of two trees (10 cm above the ground). Trunk chambers consist of a flexible polymethyl methacrylate cylindrical structure placed around a trunk portion 20 cm long. Air tightness is ensured by two rubber seals (at the top and bottom of the structure). The trunk chambers were covered with an insulated aluminum sheet to avoid light and any increase in temperature. The two trunk- and four soil-chamber effluxes were measured sequentially every 30 minutes.

2.3.2. Profiles of $[CO_2]$, $\delta^{13}C$-CO_2, SWC and T

We measured the soil CO_2 concentration $[CO_2]$ and its isotopic signature $\delta^{13}C$-CO_2 profiles using a system set up by Parent et al. (2013) based on a membrane tube technique (Flechard et al., 2007; Gut et al., 1998) which allows gas concentration equilibrium between the internal and external atmosphere. In October 2009, two parallel trenches were dug and four polypropylene tubes (1.5 m long) with gas-permeable porous walls (Accurel PPV8/2) were inserted horizontally through the soil between the trenches and spaced horizontally 40 cm apart from each other at depths of 0 (just under the litter), 5, 10, 20 and 40 cm. In July 2011, four additional Accurel tubes were dropped on the litter layer. The porous tubes were extended with Synflex® tubing. The four Synflex® tubes coming from one depth were connected together at their two ends that were also connected to form one closed loop per depth. In each closed loop system, the temporal changes in $[CO_2]$ were continuously measured by an infrared CO_2 analyzer (GMT 222 Vaisala Oyj, Helsinki, Finland).

Biogeosciences Discuss., doi:10.5194/bg-2016-194, 2016
Manuscript under review for journal Biogeosciences
Published: 17 May 2016

A small amount of air was sampled from each closed loop sequentially every 30 minutes with a solenoid-valve selection system. These samples were then diluted with zero-CO_2 air before being passed through the TDLAS for $\delta^{13}C$-CO_2 measurement. To compensate for the pressure deficit caused by sampling air from the closed loops, the same amount of fresh air was injected at a point located before the passage into the Accurel tube. Previous tests have demonstrated the efficiency of this procedure (Parent et al., 2013). The TDLAS was calibrated every 5 min with three standard gases covering the range of [CO_2] and $\delta^{13}C$-CO_2 values encountered during the sampling campaign. Parent et al. (2013) provide more details about this system and the tests proving its reliability.

We used thermocouples (constantan-copper) to record the temperature profile every 30 minutes at 0, 5, 10, 20 and 40 cm in depth and volumetric soil moisture sensors inserted horizontally at 5, 10, 20 and 40 cm depth (Theta Probe ML1, Delta-T Devices, Cambridge UK) to determine the SWC profile every 30 minutes. Output from the probes was corrected according to a site-specific calibration which was performed in the laboratory.

Continuous vertical profiles of the variables ([CO_2] and $\delta^{13}C$-CO_2, T and SWC) were obtained at each time step by cubic interpolation between the measurement points. Values at section mid-depth were used for each section. However, an uncertainty persisted as to the actual average depth of the topmost set of 4 tubes in the soil, which was especially significant in relative value (absolute error: 1.1 cm and relative error: 22%). Since we were considering purely diffusive transport, an accurate knowledge of this depth was particularly necessary; we therefore fitted the upper-tube average depth (around 5 cm) so that the diffusive estimated flux at the soil surface matched the F_s measurements.

2.3.3. Auxiliary measurements

The Hesse experimental forest station is fully equipped for measuring the main meteorological variables and for calculating the net CO_2, H_2O and energy fluxes between the forest and the atmosphere following the eddy covariance method (Longdoz et al., 2008). Half-hour mean air temperature (Tair, °C), vapor pressure deficit (VPD, hPa), atmospheric pressure (Pa, hPa) and photosynthetic photon flux density (PPFD, µmol m^{-2} s^{-1}) were determined with an HMP155 Vaisala HUMICAP® (Vaisala Inc., Helsinki, Finland; for Tair and VPD), a 144SC0811-PCB Baro (Sensortechnics, Mansfield, USA) and a PQS1 (Kipp & Zonen B.V., Delft, The Netherlands), respectively. The eddy covariance system was composed of an R3-50 (Gill Instruments, Lymington, UK) and an infrared gas analyzer Li-Cor 6262 (Li-Cor Inc., Lincoln, NE, USA). Net CO_2 ecosystem exchange (NEE, µmol m^{-2} s^{-1}) and evapotranspiration (ET, mmol m^{-2} s^{-1}) were post-processed following the Euroflux methodology (Aubinet et al., 2000) and the procedure by Longdoz et al. (2008). The partitioning of NEE into gross primary production (GPP) and ecosystem respiration (R_{eco}) was performed following the Reischtein method (Reichstein, 2005). Inherent water use efficiency (IWUE) at the ecosystem level was calculated from daytime integrated values of GPP and ET, and mean daylight VPD, according to Beer et al. (2009):

$$\mathrm{IWUE} = {\mathrm{GPP} \times \mathrm{VPD}}/{\mathrm{ET}} \quad [9]$$

Biogeosciences Discuss., doi:10.5194/bg-2016-194, 2016
Manuscript under review for journal Biogeosciences
Published: 17 May 2016

2.4. Profiles of air-filled porosities and soil diffusion coefficients

The total porosity of intact soil samples was determined by vacuum pycnometry (Maier et al., 2010). Four undisturbed soil cores (200 cm^3, 5 cm in height) were extracted at 0–5, 10–15, 20–25 and 40–45 cm depth. Air-filled porosity (ε) was obtained from the difference between total porosity and volumetric water content. One ε value was assigned to each section in FGA according to the depth of the section.

The effective soil diffusion coefficient (Ds) was estimated every centimeter as a function of the free air CO_2 diffusion coefficient in standard conditions (D_0 = 1.47×10^{-5} m^2 s^{-1} at 293.15 K and 101.3 Pa), atmospheric pressure (Pa, [Pa]), temperature at the corresponding depth (T [K]) and the relative soil diffusion coefficient (D_r= D_s/D_0 defined as the tortuosity factor) following Campbell (1985):

$$D_s = D_r \times D_0 \times \left(\frac{T}{293.15}\right)^{1.75} \times \frac{101.3}{Pa} \quad [10]$$

Atmospheric pressure was supposed constant within the whole profile and equal to the value measured in the air canopy by the meteorological station. D_r is a function of SWC established in undisturbed soil cores (see above). The cores were saturated with water, then successively drained to pre-defined levels of water potential (-1, -3, -6, -16 and -30 kPa in a filter bed; -90 kPa using a pressure plate). Gas diffusivity was measured at all potentials tested between −1 and −90 kPa, following a one-chamber method similar to that of Jassal et al. (2005), with neon (Ne) as a tracer gas (see Maier et al. 2010 for detailed procedure). For each depth, a specific D_r(SWC) function was deduced by fitting a linear regression on all the data obtained from the samples taken at this depth. The D_r value for each sections in FGA was determined by introducing the SWC value of this section into one D_r(SWC) function according to the depth of the section.

The effective diffusion coefficients at the boundary between two 5-cm-thick sections, $\overline{Ds_{1,j}}$ used in Eq (3) and Eq. (4) were calculated as the harmonic average Ds on both sides (+/- 2.5 cm) of the section boundary.

2.5. Computation and analysis

Production of CO_2, $^{12}CO_2$ and $^{13}CO_2$ was calculated in each 5-cm section using an FGA script (Goffin et al., 2014) on Matlab (R2014a version) and summed for each layer: layers 1 and 2 included two 5-cm-thick soil sections, while layer 3 included 4 sections.

We focused our analyses on four periods for which the fluxes, profiles and auxiliary data were all continuously available. These periods were spread over the whole 2014 growing season and presented contrasted climatic conditions and dynamics (Table 1).

The response of F_S and P_CO_2 to temperature was evaluated on Matlab (R2014a version) by fitting a combined Q_{10} temperature function and water content function varying from 0 at minimum SWC to 1 at field capacity (already successfully used for this site by Epron et al. (1999):

Biogeosciences Discuss., doi:10.5194/bg-2016-194, 2016
Manuscript under review for journal Biogeosciences
Published: 17 May 2016

$$P, F_S = a \times \frac{SWC - SWC_{min}}{SWC_{fc} - SWC_{min}} \times \exp\left(\frac{\ln(Q_{10}) \times T}{10}\right) \quad [11]$$

where SWC_{fc} is the soil water content at field capacity (determined from laboratory measurements) and SWC_{min} the minimal measured soil water content. The coefficient a (µmol m^{-2} s^{-1}, representing P_CO_2 or F_s standardized at 0°C and SWC_{fc}), and the temperature coefficient Q_{10} (gauging P_CO_2 or F_S sensitivity to temperature) were adjusted during the fit.

3. Results

3.1. P_CO_2 and $\delta^{13}P\_CO_2$ vertical profiles and their seasonal changes

Over the four selected time periods, average P_CO_2 in the third soil layer was two to three times lower than in the upper layers (Fig.2); at least 89% of the total soil production was confined to the upper 20 cm of soil whatever the period (Fig.3). Moreover, 64 to 77% of the CO_2 was produced in the second layer during spring while the partitioning between layers 1 and 2 was more balanced during summer, with 36 to 39 % in layer 1 and 50 to 53% in layer 2.

P_CO_2 and $\delta^{13}P\_CO_2$ presented important seasonal fluctuations, especially in the two upper layers. Average P_CO_2 increased from April to August within each of the three layers: from 1.5 to 4.4 µmol m^{-2} s^{-1} (+2.9 µmol m^{-2} s^{-1}) in layer 1, from 3.6 to 5.6 µmol m^{-2} s^{-1} (+2.0 µmol m^{-2} s^{-1}) in layer 2 and from 0.4 to 1.2 µmol m^{-2} s^{-1} (+0.8 µmol m^{-2} s^{-1}) in layer 3 (Fig.2). In summer, when P_CO_2 was higher, its daily variability was also greater (see whiskers on left panels of Fig.2).

Excluding a few values in layers 1 and 3 which correspond to a particularly dry period in June 2011 or to very low flux periods, the isotopic composition of CO_2 production ranged from -30.4 ‰ to -17.5 ‰ in the first layer, from -30.3 ‰ to -26 ‰ in the second layer and from -32.6 ‰ to -22.4 ‰ in the third layer (Fig.2). During April, $\delta^{13}P\_CO_2$ in the first layer was strongly enriched ($\delta^{13}P\_CO_{2,1}$ = -23.4 ‰ on average) compared to $\delta^{13}P$ in the second layer ($\delta^{13}P\_CO_{2,2}$ = -27.8 ‰ on average) and compared to $\delta^{13}P\_CO_{2,1}$ during August ($\delta^{13}P\_CO_{2,1}$ = -25.9 ‰). The vertical profile for $\delta^{13}P\_CO_2$ was gentler in July and August with a $\delta^{13}P\_CO_{2,2}$ of -28.5 ‰ on average; in other words, relatively similar to the profile for April. $\delta^{13}P\_CO_2$ was more variable in layer 3 than in the other two layers, but these fluctuations were unreliable.

3.2. P short-term temporal variability

From April 21st to 27th, a sunny period with no rain (Fig.4b and Fig.4c), P_CO_2 showed pronounced and regular within-day fluctuations in the first and second layers (maximum difference of 0.83 ± 0.32 (SD) µmol m^{-2} s^{-1} and 1.08 ± 0.40 (SD) µmol m^{-2} s^{-1} respectively between the daily max. and min. on average over the period, Fig.4e). P_CO_2 was more stable in the third layer (0.19 ± 0.04 (SD) µmol m^{-2} s^{-1}). Soil temperature also showed regular fluctuations but within a narrow range (maximum difference of 0.8 ± 0.2 (SD) °C in layer 1 and 0.5 ± 0.1 (SD) °C in layer 2 between the daily max. and min. on average over the period, Fig.4d).

In addition to within-day fluctuations, pronounced day-to-day variations in P_CO_2 were observed, for example from August 3rd to 21st, a period with multiple rain events. Interestingly, a drop in $P\_CO_{2,2}$ was related to a drop in soil temperature and

Biogeosciences Discuss., doi:10.5194/bg-2016-194, 2016
Manuscript under review for journal Biogeosciences
Published: 17 May 2016

PPFD but with a lag of 1 or 2 days. Minimum PPFD and soil temperature occurred on day-of-year (DOY) 221 and 223 respectively, whereas minimum $P\_CO_{2,2}$ was not observed until DOY 224. It is particularly notable that $P\_CO_{2,1}$ (decrease from 7.1 µmol m^{-2} s^{-1} on DOY 221 to 1.9 µmol m^{-2} s^{-1} on DOY 224) and $\delta^{13}P\_CO_{2,1}$ (enrichment from -27.7 ‰ to -21.7 ‰ between the same dates, Fig.4k and Fig.4l) showed an opposite trend.

3.3. Temperature sensitivity of CO_2 production

On the overall data set combining the half-hour values for the four study periods, we used an exponential function of T multiplied by a linear function varying from 1 to 0 when SWC declined (equation 11) to test P_CO_2 dependence on T and SWC.

Production in each of layers 1 and 2 was best explained with dependence on the temperature and soil water content measured within that layer compared to dependence on variables measured within another layer. For the third layer, production levels were too weak and presented such narrow fluctuations that it was impossible to fit any satisfactory equation. Exponential fits of P_CO_2 against temperature without taking SWC into account generated unrealistic Q_{10} values (> 10), probably because of the narrow range of investigated temperatures (10.8°C to 18.2°C at 5 cm depth over the season) and the covariance of T with other factors influencing P_CO_2 processes. When SWC was included in the equation, more realistic Q_{10} values were obtained (Table 2) and the value determined for F_S standardized at 0°C when soil water content is at field capacity, was roughly the sum of the P_CO_2 obtained for the first and the second layer under the same conditions (Table 2, parameter a in Eqn. 11). The Q_{10} of P_CO_2 was significantly higher in the second layer compared to the first layer, and to the Q_{10} of F_S.

3.4. Temporal variability of $\delta^{13}P\_CO_2$

Throughout the whole dataset, the distribution of $\delta^{13}F_s$ was shifted towards more positive values compared to $\delta^{13}F_t$ (Fig.5a). In the soil, $\delta^{13}P\_CO_{2,1}$ exhibited a widely spread frequency distribution with a log-normal shape from -28.5 ‰ to -22.8 ‰ extending additionally toward enriched values (up to -19.8 ‰, Figure 5b). $\delta^{13}P\_CO_{2,3}$ and $\delta^{13}P\_CO_{2,2}$ distributions were normal-shaped, though the $\delta^{13}P\_CO_{2,2}$ distribution was narrower than the $\delta^{13}P\_CO_{2,3}$ distribution, and closer to the frequency distribution of $\delta^{13}F_t$ (Fig.5c and Fig.5d).

3.5. Relationship between soil production and canopy activity

The second layer was the largest contributor to total soil production (more than 50% of the total emitted CO_2). Furthermore, different anomalies were identified for $\delta^{13}P\_CO_2$ in the first layer (non-reliable variability due to atmospheric pollution, see section 4.2.) and in the third layer (low $P\_CO_{2,3}$ intensity leading to indeterminate or beyond-range values, see section 4.2.). We therefore focused our analysis on $\delta^{13}P\_CO_{2,2}$ during the longest period with a continuous set of data available (August 3rd to August 21st). During these 3 weeks, a marked day-to-day variation for $P\_CO_{2,2}$ (3.9 to 7.5 µmol m^{-2} s^{-1}) and $\delta^{13}P\_CO_{2,2}$ (-29.7 to -27.4 ‰) was observed (Fig.4k and Fig.4l) and the daily average $P\_CO_{2,2}$ and $\delta^{13}P\_CO_{2,2}$ were strongly correlated, with an enrichment in ^{13}C when production increased (Fig.6a).

Biogeosciences Discuss., doi:10.5194/bg-2016-194, 2016
Manuscript under review for journal Biogeosciences
Published: 17 May 2016

Daily average $\delta^{13}P\_CO_{2,2}$ was correlated with the previous day's gross primary production (GPP, R=0.51), evapotranspiration (ET, R=0.45), and even more closely with inherent water use efficiency (IWUE, R=0.67, Fig.7). A simple multivariate linear regression with the IWUE of the previous day and the SWC of the current day explained 76% of the day-to-day variation in $\delta^{13}P\_CO_{2,2}$ (Fig.6b).

4. Discussion

4.1. The production of CO_2 and its vertical profile

The production values we found are in agreement with the soil CO_2 effluxes already published for this site (Epron et al., 1999; Ngao et al., 2012), except for values in June 2011 when P_CO_2 determined with FGA resulted in a few incoherent negative values in the first and third layers (Fig.2b). For the first layer, this may have been due to the rather dry period that occurred at that time (Table 1); large air-filled porosity may have favored transport through the top soil via processes other than diffusion (advection and dispersion) (Bowling and Massman, 2011; Flechard et al., 2007; Risk et al., 2008). This situation could have caused atmospheric and soil air to mix in the first centimeters, thus leading to a very low (even inverted) vertical gradient in CO_2 concentrations. Under such conditions, fluxes computed with FGA (where only diffusion transport is considered) could be underestimated and even negative. Negative production values in the third layer occurred when the concentration gradient was within the measurement uncertainties of the analyzer.

The vertical P_CO_2 profile calculated with FGA showed that 90 % of CO_2 production occurs in the two first layers (Fig.3), in agreement with Goffin et al. (2014) and Jassal et al. (2005) who showed that 75% of the soil CO_2 efflux comes from the top 20 cm in two other temperate forests. This is consistent with the vertical distribution of roots and soil organic matter (SOM); more than 65% of the roots and 73% of SOM are located in the upper 20 cm (Fig.1). The low contribution of the third layer to total soil P_CO_2 can be explained by a lower root biomass (less than one third of the root biomass was in this layer) and by stronger physical protection of SOM from microbial attack since the deep soil was composed of more than 30% clay (Baldock and Skjemstad, 2000; Lützow et al., 2006).

Temperature has been recognized as the main environmental driver of seasonal variations in soil CO_2 efflux in temperate ecosystems (Davidson et al., 2006a; Kätterer et al., 1998; Raich et al., 2002). In this study, when both temperature (T) and soil water content (SWC) were combined together in a single empirical equation, variations in CO_2 production could be satisfactorily simulated (Table 2) when fitted over the four study periods from spring to summer. The computed Q_{10} values were high (3.3 and 5.3), higher than those expected for root and microbial respiration (2 to 3, Jenkins and Adams, 2011; Lloyd and Taylor, 1994; Ryan et al., 1996; Zogg et al., 1996) but remained within the range of published values for soil CO_2 efflux in temperate forests (Borken et al., 2002; Davidson et al., 1998; Epron et al., 1999; Janssens and Pilegaard, 2003). Previously, high Q_{10} values observed for soil CO_2 efflux have often been blamed on a mismatch between the depth where soil temperature is measured and the depth where CO_2 production occurs. Indeed, when temperature is measured below CO_2 production, and because the seasonal range of soil temperature decreases with depth (Hirano et al., 2003; Pavelka et al.,

Biogeosciences Discuss., doi:10.5194/bg-2016-194, 2016
Manuscript under review for journal Biogeosciences
Published: 17 May 2016

2007), an overestimation of temperature sensitivity (Q_{10}) is needed to reproduce P_CO_2 variability. In our study, the Q_{10} of the soil CO_2 efflux matched the expected intrinsic value (2.2), even though high Q_{10} (5.3) values were calculated for the second layer and, to a lesser extent, for the first layer (Q_{10} = 3.3). Because we used the temperature measured in the same layer where CO_2 production was computed, the high Q_{10} values cannot be related to a mismatch between P_CO_2 source and measurement depth. These high values are therefore most likely due to the confounding effects of T with other abiotic drivers (PPFD) or/and to changes in basal activity of either the autotrophic or heterotrophic source at a seasonal scale (Epron et al. 2000). For example, root growth peaks in late spring and early summer, and C allocation to soil CO_2 efflux varies seasonally and peaks in July (demonstrated by pulse labeling tree photosynthesis with ^{13}C, Epron et al. 2011).

At shorter time scales (within-day, day-to-day), the variation in soil temperature was too narrow to account for variations in production. In addition, the lag between the decrease in temperature and the decrease in production, as seen in August (Fig.4j and Fig.4k), suggests that temperature is not the main driver of day-to-day variations in CO_2 production. The next section provides information about potential factors affecting these variations.

4.2. Isotope composition of CO_2 production

The isotopic composition of CO_2 produced throughout the season we estimated was within the range reported in the literature (Bowling et al., 2008; Goffin et al., 2014). The CO_2 produced in the first layer ($\delta^{13}P\_CO_{2,1}$) was more enriched than the soil CO_2 efflux ($\delta^{13}F_S$), while the CO_2 produced in the second and third layers ($\delta^{13}P\_CO_{2,2}$ or $\delta^{13}P\_CO_{2,3}$) was more depleted (Fig.5). While the opposite trend for $P\_CO_{2,1}$ and $\delta^{13}P\_CO_{2,1}$ may attest to the presence of a depleted source that increasingly supplies layer-1 production, it is more likely that $\delta^{13}P\_CO_{2,1}$ and $P\_CO_{2,1}$ were simultaneously and respectively over- and underestimated when upper soil CO_2 was mixed with atmospheric air during turbulence events. Effectively, any input of atmospheric CO_2 by advection or dispersion (with lower concentrations and higher δ^{13}) would generate artifacts on P_CO_2 and $\delta^{13}P\_CO_2$ estimations because only diffusion is considered in FGA (Kayler et al., 2010). Mixing soil and atmospheric air could also explain the enrichment of $\delta^{13}P\_CO_{2,1}$ compared to $\delta^{13}F_S$, and the fact that, while the distribution of $\delta^{13}P\_CO_{2,2}$ and $\delta^{13}P\_CO_{2,3}$ was normal, the distribution of $\delta^{13}P\_CO_{2,1}$ formed a lognormal shape. Finally, a few values computed for the third layer were beyond the expected range, which could result from the greater uncertainties when calculating the ratio of ^{13}C to ^{12}C production when values are close to 0.

The isotopic composition of the CO_2 produced in the second soil layer ($\delta^{13}P\_CO_{2,2}$) was close to the isotopic composition of tree trunk CO_2 efflux ($\delta^{13}F_t$). The similarity between $\delta^{13}P\_CO_{2,2}$ and $\delta^{13}F_t$ distributions suggests that autotrophic activity largely contributes to CO_2 production in this second layer. This layer contained the same amount of roots as the two other layers, but probably a lower amount of labile organic matter than the first layer (Braakhekke et al., 2011; Rumpel et al., 2002). At the daily time scale, $\delta^{13}P\_CO_{2,2}$ was well correlated with the IWUE measured the day before (Fig.7); this attests to a link between canopy activity and soil autotrophic production in the second layer. Indeed, the connection between the day-to-day fluctuations in $\delta^{13}P\_CO_{2,2}$ and canopy activity is related to fractionation occurring during photosynthesis, carbohydrate transport and respiration (Griffis, 2013). Carbon isotope discrimination during photosynthesis depends on the

Biogeosciences Discuss., doi:10.5194/bg-2016-194, 2016
Manuscript under review for journal Biogeosciences
Published: 17 May 2016

intercellular carbon dioxide concentrations in leaves, which is linked to WUE; any change in water use efficiency changes photosynthetic carbon isotope discrimination (Farquhar et al. 1982) and impacts the $\delta^{13}C$ of the photosynthetic products that fuel respiration (Ekblad and Högberg, 2001; Gessler et al., 2007). The fluctuations in $\delta^{13}P\_CO_{2,2}$ we found therefore reflect temporal climate-driven variations in photosynthetic carbon isotope discrimination, and the one-day delay of $\delta^{13}P\_CO_{2,2}$ response to IWUE is coherent with the time necessary for the photosynthates to be transported belowground. Pulse labeling trees with ^{13}C has revealed a lag between tree crown assimilation and soil CO_2 efflux of about 0.5 -1.5 days for the Hesse site (Plain et al. 2009; Epron et al. 2011). This is also consistent with the lagged decline in $P\_CO_{2,2}$ after a decrease in photon flux density in August (Fig.4i: DOY 219 and Fig.4k: DOY 221). Moreover, $P\_CO_{2,2}$ and $\delta^{13}P\_CO_{2,2}$ were strongly correlated in our study, with enrichment occurring when production increased (Fig.6). One explanation is that a temporal increase in gross primary production may stimulate root and rhizospheric respiration with a 24h delay, and that high rates of leaf CO_2 assimilation accounting for the increase in GPP decreases intercellular carbon dioxide concentrations in the leaves, thus decreasing carbon isotope discrimination during photosynthesis (Seibt et al., 2008). Furthermore, we performed a simple multivariate linear regression between $\delta^{13}P\_CO_{2,2,}$ the IWUE of the previous day and the SWC of the current day which suggests that, in addition to an autotrophic source related to lag variations in IWUE, a source responsive to short-term changes in soil water content contributes to CO_2 production in the second layer. Microbial respiration is highly sensitive to local changes in SWC (Moyano et al., 2012; Orchard and Cook, 1983) and is thought to respond faster to fluctuation in SWC than root respiration. We therefore hypothesize that heterotrophic sources also contribute to CO_2 production in the second soil layer, though our data did not allow us to quantify the relative contribution of autotrophic and heterotrophic sources to CO_2 production.

5. Conclusion

The combination of FGA with high frequency measurements of soil CO_2 isotopic composition allowed us to determine the vertical distribution of CO_2 production (P_CO_2) and its isotopic composition ($\delta^{13}P\_CO_2$), especially during calm weather periods with low atmospheric turbulence. Most CO_2 production (90 %) occurred in the upper 20 cm of the soil and was related to root and SOM vertical distributions. The P_CO_2 seasonal variability of each layer was best related to its own temperature, with significant differences in temperature sensitivities among the layers. Significant day-to-day fluctuations were observed for P_CO_2 and $\delta^{13}P\_CO_2$, especially in the second layer, but the variation in soil temperatures was too narrow to account for these variations. However, these fluctuations seems to be due to a large contribution from autotrophic sources, since a strong link between P_CO_2, $\delta^{13}P\_CO_2$ and canopy activity (through inherent water use efficiency) was found for the second layer. In addition, heterotrophic sources responding to rapid changes in soil water content also contributed to CO_2 production in this layer. We were not able to separate the contribution of autotrophic and heterotrophic sources to CO_2 production because of their temporal variability and because the differences in their isotopic signatures were too small.

355 Despite this limitation, the isotopic flux-gradient approach gave consistent and promising results. Production estimates in the top soil layers will be further improved in the future by accounting for turbulent advection and dispersion processes.

Acknowledgment

Data can be made available upon request from the corresponding author.

Financial support was provided by the Université de Lorraine, the Conseil Régional de Lorraine, the French National
360 Research Agency through the Laboratory of Excellence ARBRE (ANR-11-LABX-0002-01) and the GIP ECOFOR.

We are particularly grateful to Florian Parent for the test and validation of the method for $\delta^{13}C\text{-}CO_2$ soil profile measurements and to Martin Maier for the laboratory measurements of porosity and the diffusive coefficient.

We also thank Patrick Gross, Pascal Courtois, Jean-Marie-Gioria and Bernard Clerc for their technical assistance in the field.

References

365 Aubinet, M., Grelle, A., Ibrom, A., Rannik, Ü., Moncrieff, J., Foken, T., Kowalski, A. S., Martin, P. H., Berbigier, P., Bernhofer, C., Clement, R., Elbers, J., Granier, A., Grünwald, T., Morgenstern, K., Pilegaard, K., Rebmann, C., Snijders, W., Valentini, R. and Vesala, T.: Estimates of the annual net carbon and water exchange of forests: the EUROFLUX methodology., Adv. Ecol. Res., 30, 113–175, doi:10.1016/S0065-2504(08)60018-5, 2000.

Baldock, J. A. and Skjemstad, J. O.: Role of the soil matrix and minerals in protecting natural organic materials against
370 biological attack, Org. Geochem., 31(7–8), 697–710, doi:10.1016/S0146-6380(00)00049-8, 2000.

Beer, C., Ciais, P., Reichstein, M., Baldocchi, D., Law, B. E., Papale, D., Soussana, J.-F., Ammann, C., Buchmann, N., Frank, D., Gianelle, D., Janssens, I. A., Knohl, A., Köstner, B., Moors, E., Roupsard, O., Verbeeck, H., Vesala, T., Williams, C. A. and Wohlfahrt, G.: Temporal and among-site variability of inherent water use efficiency at the ecosystem level, Glob. Biogeochem. Cycles, 23(2), GB2018, doi:10.1029/2008GB003233, 2009.

375 Boone, R. D., Nadelhoffer, K. J., Canary, J. D. and Kaye, J. P.: Roots exert a strong influence on the temperature sensitivity of soil respiration, Nature, 396(6711), 570–572, doi:10.1038/25119, 1998.

Borken, W., Xu, Y.-J., Davidson, E. A. and Beese, F.: Site and temporal variation of soil respiration in European beech, Norway spruce, and Scots pine forests, Glob. Change Biol., 8(12), 1205–1216, doi:10.1046/j.1365-2486.2002.00547.x, 2002.

380 Bowling, D. R. and Massman, W. J.: Persistent wind-induced enhancement of diffusive CO2 transport in a mountain forest snowpack, J. Geophys. Res. Biogeosciences, 116(G4), G04006, doi:10.1029/2011JG001722, 2011.

Bowling, D. R., McDowell, N. G., Bond, B. J., Law, B. E. and Ehleringer, J. R.: 13C content of ecosystem respiration is linked to precipitation and vapor pressure deficit, Oecologia, 131(1), 113–124, doi:10.1007/s00442-001-0851-y, 2002.

Bowling, D. R., Pataki, D. E. and Randerson, J. T.: Carbon isotopes in terrestrial ecosystem pools and CO2 fluxes, New
385 Phytol., 178(1), 24–40, doi:10.1111/j.1469-8137.2007.02342.x, 2008.

Braakhekke, M. C., Beer, C., Hoosbeek, M. R., Reichstein, M., Kruijt, B., Schrumpf, M. and Kabat, P.: SOMPROF: A vertically explicit soil organic matter model, Ecol. Model., 222(10), 1712–1730, doi:10.1016/j.ecolmodel.2011.02.015, 2011.

Campbell, G. S.: Soil Physics with BASIC: Transport Models for Soil-Plant Systems, Elsevier., 1985.

Cerling, T. E., Solomon, D. K., Quade, J. and Bowman, J. R.: On the isotopic composition of carbon in soil carbon dioxide, Geochim. Cosmochim. Acta, 55(11), 3403–3405, doi:10.1016/0016-7037(91)90498-T, 1991.

Conant, R. T., Ryan, M. G., Ågren, G. I., Birge, H. E., Davidson, E. A., Eliasson, P. E., Evans, S. E., Frey, S. D., Giardina, C. P., Hopkins, F. M., Hyvönen, R., Kirschbaum, M. U. F., Lavallee, J. M., Leifeld, J., Parton, W. J., Megan Steinweg, J., Wallenstein, M. D., Martin Wetterstedt, J. Å. and Bradford, M. A.: Temperature and soil organic matter decomposition rates – synthesis of current knowledge and a way forward, Glob. Change Biol., 17(11), 3392–3404, doi:10.1111/j.1365-2486.2011.02496.x, 2011.

Davidson, E. A., Belk, E. and Boone, R. D.: Soil water content and temperature as independent or confounded factors controlling soil respiration in a temperate mixed hardwood forest, Glob. Change Biol., 4(2), 217–227, doi:10.1046/j.1365-2486.1998.00128.x, 1998.

Davidson, E. A., Janssens, I. A. and Luo, Y.: On the variability of respiration in terrestrial ecosystems: moving beyond Q10, Glob. Change Biol., 12(2), 154–164, doi:10.1111/j.1365-2486.2005.01065.x, 2006a.

Davidson, E. A., Savage, K. E., Trumbore, S. E. and Borken, W.: Vertical partitioning of CO2 production within a temperate forest soil, Glob. Change Biol., 12(6), 944–956, doi:10.1111/j.1365-2486.2005.01142.x, 2006b.

Ekblad, A. and Högberg, P.: Natural abundance of 13C in CO2 respired from forest soils reveals speed of link between tree photosynthesis and root respiration, Oecologia, 127(3), 305–308, doi:10.1007/s004420100667, 2001.

Ekblad, A., Boström, B., Holm, A. and Comstedt, D.: Forest soil respiration rate and δ13C is regulated by recent above ground weather conditions, Oecologia, 143(1), 136–142, doi:10.1007/s00442-004-1776-z, 2004.

Epron, D.: Separating autotrophic and heterotrophic components of soil respiration: lessons learned from trenching and related root-exclusion experiments, in Soil Carbon Dynamics, Cambridge University Press. [online] Available from: http://dx.doi.org/10.1017/CBO9780511711794.009, 2009.

Epron, D., Farque, L., Lucot, É. and Badot, P.-M.: Soil CO2 efflux in a beech forest: dependence on soil temperature and soil water content, Ann. For. Sci., 56(3), 221–226, 1999.

Epron, D., Dantec, V. L., Dufrene, E. and Granier, A.: Seasonal dynamics of soil carbon dioxide efflux and simulated rhizosphere respiration in a beech forest, Tree Physiol., 21(2-3), 145–152, doi:10.1093/treephys/21.2-3.145, 2001.

Epron, D., Ngao, J., Dannoura, M., Bakker, M. R., Zeller, B., Bazot, S., Bosc, A., Plain, C., Lata, J. C., Priault, P. and others: Seasonal variations of belowground carbon transfer assessed by in situ 13CO2 pulse labelling of trees, Biogeosciences, 8(5), 1153–1168, 2011.

Fang, C. and Moncrieff, J. B.: A model for soil CO2 production and transport 1:, Agric. For. Meteorol., 95(4), 225–236, doi:10.1016/S0168-1923(99)00036-2, 1999.

Fessenden, J. E. and Ehleringer, J. R.: Temporal variation in δ13C of ecosystem respiration in the Pacific Northwest: links to moisture stress, Oecologia, 136(1), 129–136, doi:10.1007/s00442-003-1260-1, 2003.

Flechard, C. R., Neftel, A., Jocher, M., Ammann, C., Leifeld, J. and Fuhrer, J.: Temporal changes in soil pore space CO2 concentration and storage under permanent grassland, Agric. For. Meteorol., 142(1), 66–84, doi:10.1016/j.agrformet.2006.11.006, 2007.

Gessler, A., Keitel, C., Kodama, N., Weston, C., Winters, A. J., Keith, H., Grice, K., Leuning, R. and Farquhar, G. D.: δ13C of organic matter transported from the leaves to the roots in Eucalyptus delegatensis: short-term variations and relation to respired CO2, Funct. Plant Biol., 34(8), 692–706, 2007.

Goffin, S., Aubinet, M., Maier, M., Plain, C., Schack-Kirchner, H. and Longdoz, B.: Characterization of the soil CO2 production and its carbon isotope composition in forest soil layers using the flux-gradient approach, Agric. For. Meteorol., 188, 45–57, 2014.

Granier, A., Ceschia, E., Damesin, C., Dufrêne, E., Epron, D., Gross, P., Lebaube, S., Le Dantec, V., Le Goff, N., Lemoine, D., Lucot, E., Ottorini, J. M., Pontailler, J. Y. and Saugier, B.: The carbon balance of a young Beech forest, Funct. Ecol., 14(3), 312–325, doi:10.1046/j.1365-2435.2000.00434.x, 2000.

Griffis, T. J.: Tracing the flow of carbon dioxide and water vapor between the biosphere and atmosphere: A review of optical isotope techniques and their application, Agric. For. Meteorol., 174–175, 85–109, doi:10.1016/j.agrformet.2013.02.009, 2013.

Griffis, T. J., Baker, J. M., Sargent, S. D., Tanner, B. D. and Zhang, J.: Measuring field-scale isotopic CO2 fluxes with tunable diode laser absorption spectroscopy and micrometeorological techniques, Agric. For. Meteorol., 124(1–2), 15–29, doi:10.1016/j.agrformet.2004.01.009, 2004.

Gut, A., Blatter, A., Fahrni, M., Lehmann, B. E., Neftel, A. and Staffelbach, T.: A new membrane tube technique (METT) for continuous gas measurements in soils, Plant Soil, 198(1), 79–88, doi:10.1023/A:1004277519234, 1998.

Hirano, T., Kim, H. and Tanaka, Y.: Long-term half-hourly measurement of soil CO2 concentration and soil respiration in a temperate deciduous forest, J. Geophys. Res. Atmospheres, 108(D20), 4631, doi:10.1029/2003JD003766, 2003.

Janssens, I. A. and Pilegaard, K.: Large seasonal changes in Q10 of soil respiration in a beech forest, Glob. Change Biol., 9(6), 911–918, 2003.

Janssens, I. A., Freibauer, A., Ciais, P., Smith, P., Nabuurs, G.-J., Folberth, G., Schlamadinger, B., Hutjes, R. W., Ceulemans, R. and Schulze, E.-D.: Europe's terrestrial biosphere absorbs 7 to 12% of European anthropogenic CO2 emissions, Science, 300(5625), 1538–1542, 2003.

Jassal, R., Black, A., Novak, M., Morgenstern, K., Nesic, Z. and Gaumont-Guay, D.: Relationship between soil CO2 concentrations and forest-floor CO2 effluxes, Agric. For. Meteorol., 130(3–4), 176–192, doi:10.1016/j.agrformet.2005.03.005, 2005.

Jassal, R. S., Black, T. A., Drewitt, G. B., Novak, M. D., Gaumont-Guay, D. and Nesic, Z.: A model of the production and transport of CO2 in soil: predicting soil CO2 concentrations and CO2 efflux from a forest floor, Agric. For. Meteorol., 124(3–4), 219–236, doi:10.1016/j.agrformet.2004.01.013, 2004.

Jenkins, M. E. and Adams, M. A.: Respiratory quotients and Q10 of soil respiration in sub-alpine Australia reflect influences of vegetation types, Soil Biol. Biochem., 43(6), 1266–1274, doi:10.1016/j.soilbio.2011.02.017, 2011.

Jong, E. D. and Schappert, H. J. V.: Calculation of soil respiration and activity from CO2 profiles in the soil, Soil Sci., 113(5), 328–333, 1972.

Karhu, K., Auffret, M. D., Dungait, J. A. J., Hopkins, D. W., Prosser, J. I., Singh, B. K., Subke, J.-A., Wookey, P. A., Ågren, G. I., Sebastià, M.-T., Gouriveau, F., Bergkvist, G., Meir, P., Nottingham, A. T., Salinas, N. and Hartley, I. P.: Temperature sensitivity of soil respiration rates enhanced by microbial community response, Nature, 513(7516), 81–84, doi:10.1038/nature13604, 2014.

Kätterer, T., Reichstein, M., Andrén, O. and Lomander, A.: Temperature dependence of organic matter decomposition: a critical review using literature data analyzed with different models, Biol. Fertil. Soils, 27(3), 258–262, doi:10.1007/s003740050430, 1998.

Kayler, Z. E., Sulzman, E. W., Rugh, W. D., Mix, A. C. and Bond, B. J.: Characterizing the impact of diffusive and advective soil gas transport on the measurement and interpretation of the isotopic signal of soil respiration, Soil Biol. Biochem., 42(3), 435–444, doi:10.1016/j.soilbio.2009.11.022, 2010.

Kuzyakov, Y. and Gavrichkova, O.: REVIEW: Time lag between photosynthesis and carbon dioxide efflux from soil: a review of mechanisms and controls, Glob. Change Biol., 16(12), 3386–3406, doi:10.1111/j.1365-2486.2010.02179.x, 2010.

Lai, C.-T., Ehleringer, J. R., Schauer, A. J., Tans, P. P., Hollinger, D. Y., Paw U, K. T., Munger, J. W. and Wofsy, S. C.: Canopy-scale δ13C of photosynthetic and respiratory CO2 fluxes: observations in forest biomes across the United States, Glob. Change Biol., 11(4), 633–643, doi:10.1111/j.1365-2486.2005.00931.x, 2005.

Law, B. E., Ryan, M. G. and Anthoni, P. M.: Seasonal and annual respiration of a ponderosa pine ecosystem, Glob. Change Biol., 5(2), 169–182, doi:10.1046/j.1365-2486.1999.00214.x, 1999.

Lloyd, J. and Taylor, J. A.: On the Temperature Dependence of Soil Respiration, Funct. Ecol., 8(3), 315–323, doi:10.2307/2389824, 1994.

Longdoz, B., Gross, P. and Granier, A.: Multiple quality tests for analysing CO2 fluxes in a beech temperate forest, Biogeosciences, 5(3), 719–729, doi:10.5194/bg-5-719-2008, 2008.

Lützow, M. v., Kögel-Knabner, I., Ekschmitt, K., Matzner, E., Guggenberger, G., Marschner, B. and Flessa, H.: Stabilization of organic matter in temperate soils: mechanisms and their relevance under different soil conditions – a review, Eur. J. Soil Sci., 57(4), 426–445, doi:10.1111/j.1365-2389.2006.00809.x, 2006.

Maier, M., Schack-Kirchner, H., Hildebrand, E. E. and Holst, J.: Pore-space CO2 dynamics in a deep, well-aerated soil, Eur. J. Soil Sci., 61(6), 877–887, doi:10.1111/j.1365-2389.2010.01287.x, 2010.

Maier, M., Schack-Kirchner, H., Aubinet, M., Goffin, S., Longdoz, B. and Parent, F.: Turbulence Effect on Gas Transport in Three Contrasting Forest Soils, Soil Sci. Soc. Am. J., 76(5), 1518, doi:10.2136/sssaj2011.0376, 2012.

Marron, N., Plain, C., Longdoz, B. and Epron, D.: Seasonal and daily time course of the 13C composition in soil CO2 efflux recorded with a tunable diode laser spectrophotometer (TDLS), Plant Soil, 318(1-2), 137–151, doi:10.1007/s11104-008-9824-9, 2009.

Moyano, F. E., Vasilyeva, N., Bouckaert, L., Cook, F., Craine, J., Curiel Yuste, J., Don, A., Epron, D., Formanek, P., Franzluebbers, A., Ilstedt, U., Kätterer, T., Orchard, V., Reichstein, M., Rey, A., Ruamps, L., Subke, J.-A., Thomsen, I. K. and Chenu, C.: The moisture response of soil heterotrophic respiration: interaction with soil properties, Biogeosciences, 9(3), 1173–1182, doi:10.5194/bg-9-1173-2012, 2012.

Moyes, A. B., Gaines, S. J., Siegwolf, R. T. W. and Bowling, D. R.: Diffusive fractionation complicates isotopic partitioning of autotrophic and heterotrophic sources of soil respiration, Plant Cell Environ., 33(11), 1804–1819, doi:10.1111/j.1365-3040.2010.02185.x, 2010.

Ngao, J., Epron, D., Delpierre, N., Bréda, N., Granier, A. and Longdoz, B.: Spatial variability of soil CO2 efflux linked to soil parameters and ecosystem characteristics in a temperate beech forest, Agric. For. Meteorol., 154–155, 136–146, doi:10.1016/j.agrformet.2011.11.003, 2012.

Orchard, V. A. and Cook, F. J.: Relationship between soil respiration and soil moisture, Soil Biol. Biochem., 15(4), 447–453, doi:10.1016/0038-0717(83)90010-X, 1983.

Parent, F., Plain, C., Epron, D., Maier, M. and Longdoz, B.: A new method for continuously measuring the δ13C of soil CO2 concentrations at different depths by laser spectrometry, Eur. J. Soil Sci., 64(4), 516–525, doi:10.1111/ejss.12047, 2013.

Pavelka, M., Acosta, M., Marek, M. V., Kutsch, W. and Janous, D.: Dependence of the Q10 values on the depth of the soil temperature measuring point, Plant Soil, 292(1-2), 171–179, doi:10.1007/s11104-007-9213-9, 2007.

Peiffer, M., Le Goff, N., Nys, C., Ottorini, J.-M. and Granier, A.: Bilan d'eau, de carbone et croissances comparées de deux hêtraies de plaine, in Revue forestière française, vol. 57, pp. 201–216, Ecole nationale du génie rural, des eaux et des forêts. [online] Available from: http://cat.inist.fr/?aModele=afficheN&cpsidt=17263048 (Accessed 1 April 2016), 2005.

Plain, C., Gerant, D., Maillard, P., Dannoura, M., Dong, Y., Zeller, B., Priault, P., Parent, F. and Epron, D.: Tracing of recently assimilated carbon in respiration at high temporal resolution in the field with a tuneable diode laser absorption spectrometer after in situ 13CO2 pulse labelling of 20-year-old beech trees, Tree Physiol., 29(11), 1433–1445, doi:10.1093/treephys/tpp072, 2009.

Prévost-Bouré, N. C., Ngao, J., Berveiller, D., Bonal, D., Damesin, C., Dufrêne, E., Lata, J.-C., Dantec, V. L., Longdoz, B., Ponton, S., Soudani, K. and Epron, D.: Root exclusion through trenching does not affect the isotopic composition of soil CO2 efflux, Plant Soil, 319(1-2), 1–13, doi:10.1007/s11104-008-9844-5, 2008.

Pumpanen, J., Ilvesniemi, H. and Hari, P.: A Process-Based Model for Predicting Soil Carbon Dioxide Efflux and Concentration, Soil Sci. Soc. Am. J., 67(2), 402, doi:10.2136/sssaj2003.4020, 2003.

Pumpanen, J., Ilvesniemi, H., Kulmala, L., Siivola, E., Laakso, H., Kolari, P., Helenelund, C., Laakso, M., Uusimaa, M. and Hari, P.: Respiration in Boreal Forest Soil as Determined from Carbon Dioxide Concentration Profile, Soil Sci. Soc. Am. J., 72(5), 1187, doi:10.2136/sssaj2007.0199, 2008.

Raich, J. W., Potter, C. S. and Bhagawati, D.: Interannual variability in global soil respiration, 1980–94, Glob. Change Biol., 8(8), 800–812, doi:10.1046/j.1365-2486.2002.00511.x, 2002.

Reichstein, M.: On the separation of net ecosystem exchange into assimilation and ecosystem respiration: review and improved algorithm, Glob. Change Biol., 11(9), 1424–1439, doi:10.1111/j.1365-2486.2005.001002.x, 2005.

Risk, D., Kellman, L. and Beltrami, H.: A new method for in situ soil gas diffusivity measurement and applications in the monitoring of subsurface CO2 production, J. Geophys. Res. Biogeosciences, 113(G2), G02018, doi:10.1029/2007JG000445, 2008.

Risk, D., Nickerson, N., Phillips, C. L., Kellman, L. and Moroni, M.: Drought alters respired δ13CO2 from autotrophic, but not heterotrophic soil respiration, Soil Biol. Biochem., 50, 26–32, doi:10.1016/j.soilbio.2012.01.025, 2012.

Rumpel, C., Kögel-Knabner, I. and Bruhn, F.: Vertical distribution, age, and chemical composition of organic carbon in two forest soils of different pedogenesis, Org. Geochem., 33(10), 1131–1142, doi:10.1016/S0146-6380(02)00088-8, 2002.

Ryan, M. G. and Law, B. E.: Interpreting, measuring, and modeling soil respiration, Biogeochemistry, 73(1), 3–27, doi:10.1007/s10533-004-5167-7, 2005.

Ryan, M. G., Hubbard, R. M., Pongracic, S., Raison, R. J. and McMurtrie, R. E.: Foliage, fine-root, woody-tissue and stand respiration in Pinus radiata in relation to nitrogen status, Tree Physiol., 16(3), 333–343, doi:10.1093/treephys/16.3.333, 1996.

Seibt, U., Rajabi, A., Griffiths, H. and Berry, J. A.: Carbon isotopes and water use efficiency: sense and sensitivity, Oecologia, 155(3), 441–454, doi:10.1007/s00442-007-0932-7, 2008.

Subke, J.-A., Inglima, I. and Francesca Cotrufo, M.: Trends and methodological impacts in soil CO2 efflux partitioning: A metaanalytical review, Glob. Change Biol., 12(6), 921–943, doi:10.1111/j.1365-2486.2006.01117.x, 2006.

Suleau, M., Moureaux, C., Dufranne, D., Buysse, P., Bodson, B., Destain, J.-P., Heinesch, B., Debacq, A. and Aubinet, M.: Respiration of three Belgian crops: partitioning of total ecosystem respiration in its heterotrophic, above-and below-ground autotrophic components, Agric. For. Meteorol., 151(5), 633–643, 2011.

Vargas, R., Baldocchi, D. D., Bahn, M., Hanson, P. J., Hosman, K. P., Kulmala, L., Pumpanen, J. and Yang, B.: On the multi-temporal correlation between photosynthesis and soil CO2 efflux: reconciling lags and observations, New Phytol., 191(4), 1006–1017, doi:10.1111/j.1469-8137.2011.03771.x, 2011.

Vargas, R., Collins, S. L., Thomey, M. L., Johnson, J. E., Brown, R. F., Natvig, D. O. and Friggens, M. T.: Precipitation variability and fire influence the temporal dynamics of soil CO2 efflux in an arid grassland, Glob. Change Biol., 18(4), 1401–1411, doi:10.1111/j.1365-2486.2011.02628.x, 2012.

Werner, D., Grathwohl, P. and Höhener, P.: Review of Field Methods for the Determination of the Tortuosity and Effective Gas-Phase Diffusivity in the Vadose Zone, Vadose Zone J., 3(4), 1240, doi:10.2136/vzj2004.1240, 2004.

Wingate, L., Ogée, J., Burlett, R., Bosc, A., Devaux, M., Grace, J., Loustau, D. and Gessler, A.: Photosynthetic carbon isotope discrimination and its relationship to the carbon isotope signals of stem, soil and ecosystem respiration, New Phytol., 188(2), 576–589, doi:10.1111/j.1469-8137.2010.03384.x, 2010.

Zogg, G. P., Zak, D. R., Burton, A. J. and Pregitzer, K. S.: Fine root respiration in northern hardwood forests in relation to temperature and nitrogen availability, Tree Physiol., 16(8), 719–725, doi:10.1093/treephys/16.8.719, 1996.

Biogeosciences Discuss., doi:10.5194/bg-2016-194, 2016
Manuscript under review for journal Biogeosciences
Published: 17 May 2016

Table 1: Minimum, maximum and average soil temperature (T) and soil water content (SWC) measured at 5 cm depth, average gross primary production (GPP) and evapotranspiration (GPP) and cumulated rain over of the four selected time periods.

	T_{min} [°C]	T_{max} [°C]	T_{av} [°C]	SWC_{min} [m^3m^{-3}]	SWC_{max} [m^3m^{-3}]	SWC_{av} [m^3m^{-3}]	Rain [mm]	GPP [gC m^{-2} d^{-1}]	ET [kgH_2O m^{-2} d^{-1}]
22 – 27 April	10.8	11.4	11.1	0.24	0.27	0.25	1.2	0.6	1.34
04 – 09 June	13.2	15.2	14.4	0.12	0.14	0.13	25.4	10.2	1.91
24 – 28 July	13.3	14.8	14.1	0.20	0.22	0.21	14.4	11.3	1.28
04 – 20 August	14.0	18.2	16.3	0.13	0.20	0.17	58.4	8.3	1.88

Biogeosciences Discuss., doi:10.5194/bg-2016-194, 2016
Manuscript under review for journal Biogeosciences
Published: 17 May 2016

560 **Table 2: Estimated parameters with their standard errors for empirical models (Eqn. 11) relating soil CO_2 efflux (F_S), CO_2 production between 0 and -10 cm depth ($P\_CO_{2,1}$) or CO_2 production between -10 and -20 cm depth ($P\_CO_{2,}P_2$) and soil temperature and water content at either 5 cm depth ($P\_CO_{2,1}$) or at 15 cm depth ($P\_CO_{2,2}$ and F_S). The retained depths for soil temperature and water content were those giving the highest coefficients of determination (R^2). Parameter 'a' is F_S or P_CO_2 standardized at 0°C when soil water content is at field capacity. Q_{10} is the temperature sensitivity.**

	a (µmol m^{-2} s^{-1})	Q_{10}	R^2
F_S	0.27 ± 0.02	2.2 ± 0.1	0.56
$P\_CO_{2,1}$	0.18 ± 0.09	3.3 ± 1.2	0.62
$P\_CO_{2,2}$	0.11 ± 0.02	5.3 ± 0.7	0.67

565

Biogeosciences Discuss., doi:10.5194/bg-2016-194, 2016
Manuscript under review for journal Biogeosciences
Published: 17 May 2016

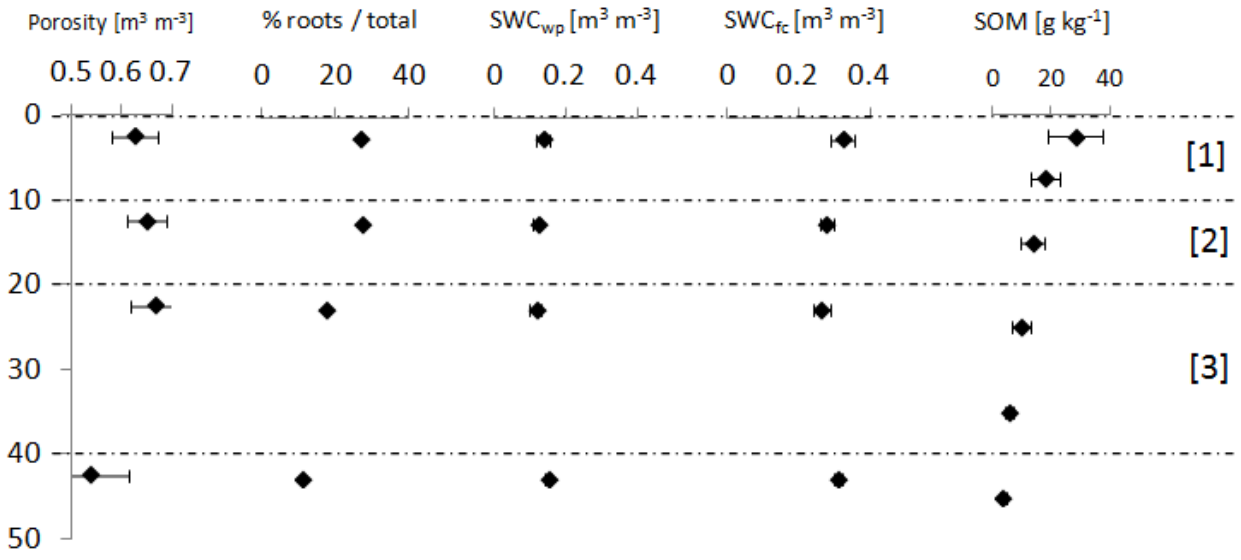

Figure 1: Vertical distribution of average total porosity (m^3 m^{-3}, the error bars correspond to the standard deviation between samples), fine root proportion (% of total root content over the profile), soil water content at wilting point (SWC_{wp}, m^3 m^{-3}), soil water content at field capacity (SWC_{fc}, m^3 m^{-3}) and SOM content in the three defined layers [1] 0 to -10 cm, [2] -10 cm to -20 cm and [3] -20 to -40 cm.

Biogeosciences Discuss., doi:10.5194/bg-2016-194, 2016
Manuscript under review for journal Biogeosciences
Published: 17 May 2016

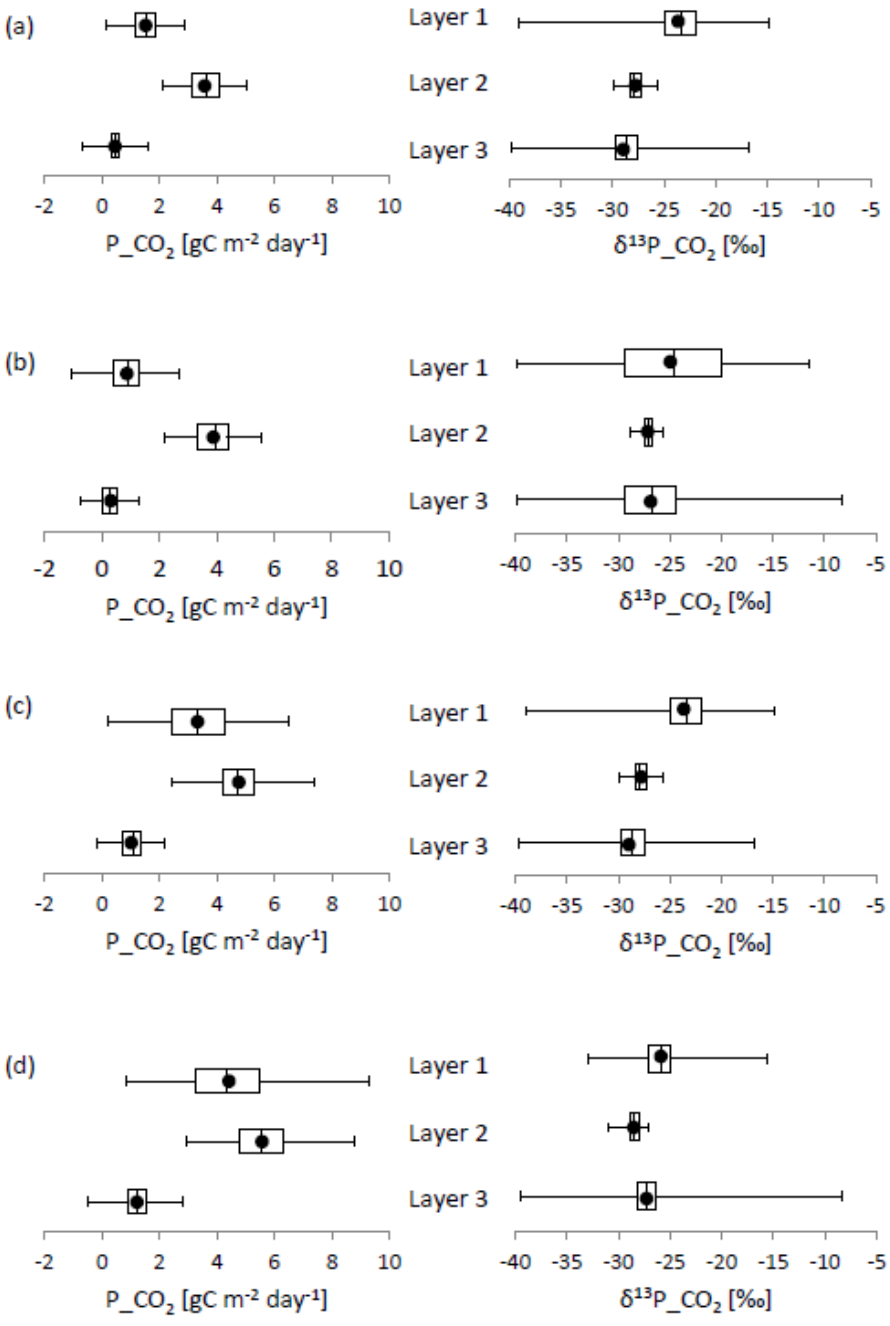

575 **Figure 2: CO_2 production (P_CO_2, left) and its isotopic signature ($\delta^{13}P\_CO_2$, right) in each layer over different time periods: (a) 21 to 27 April, (b) 03 to 10 June, (c) 22 to 29 July and (d) 03 to 21 August. The central line is the median, the central dot is the average value, the edges of the box are the 25th and 75th percentiles, and the whiskers extend to the most extreme data points. P_CO_2 and $\delta^{13}P\_CO_2$ were calculated based on measurements taken every 30 minutes.**

Biogeosciences Discuss., doi:10.5194/bg-2016-194, 2016
Manuscript under review for journal Biogeosciences
Published: 17 May 2016

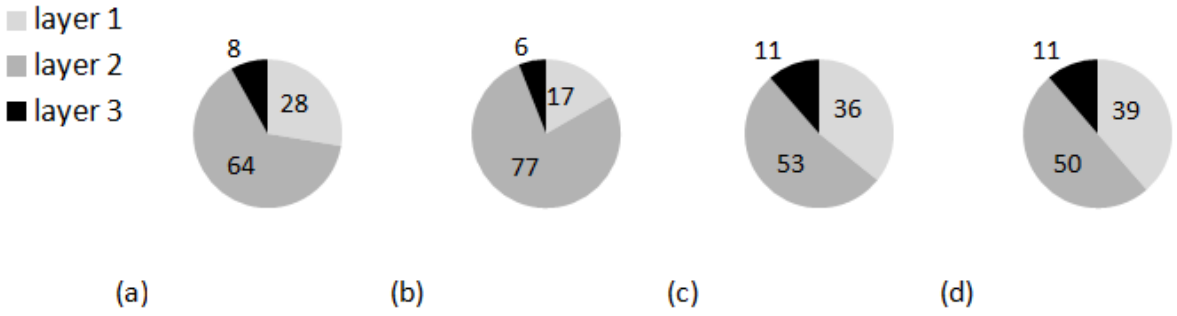

580 **Figure 3: Average contribution of each layer to total soil CO_2 production for the four different time periods (a) 21 to 27 April, (b) 03 to 10 June, (c) 22 to 29 July and (d) 03 to 21 August. Light grey = layer 1 (0 cm to -10 cm), grey = layer 2 (-10 cm to -20 cm) and black = layer 3 (-20 cm to -40 cm)**

Biogeosciences Discuss., doi:10.5194/bg-2016-194, 2016
Manuscript under review for journal Biogeosciences
Published: 17 May 2016

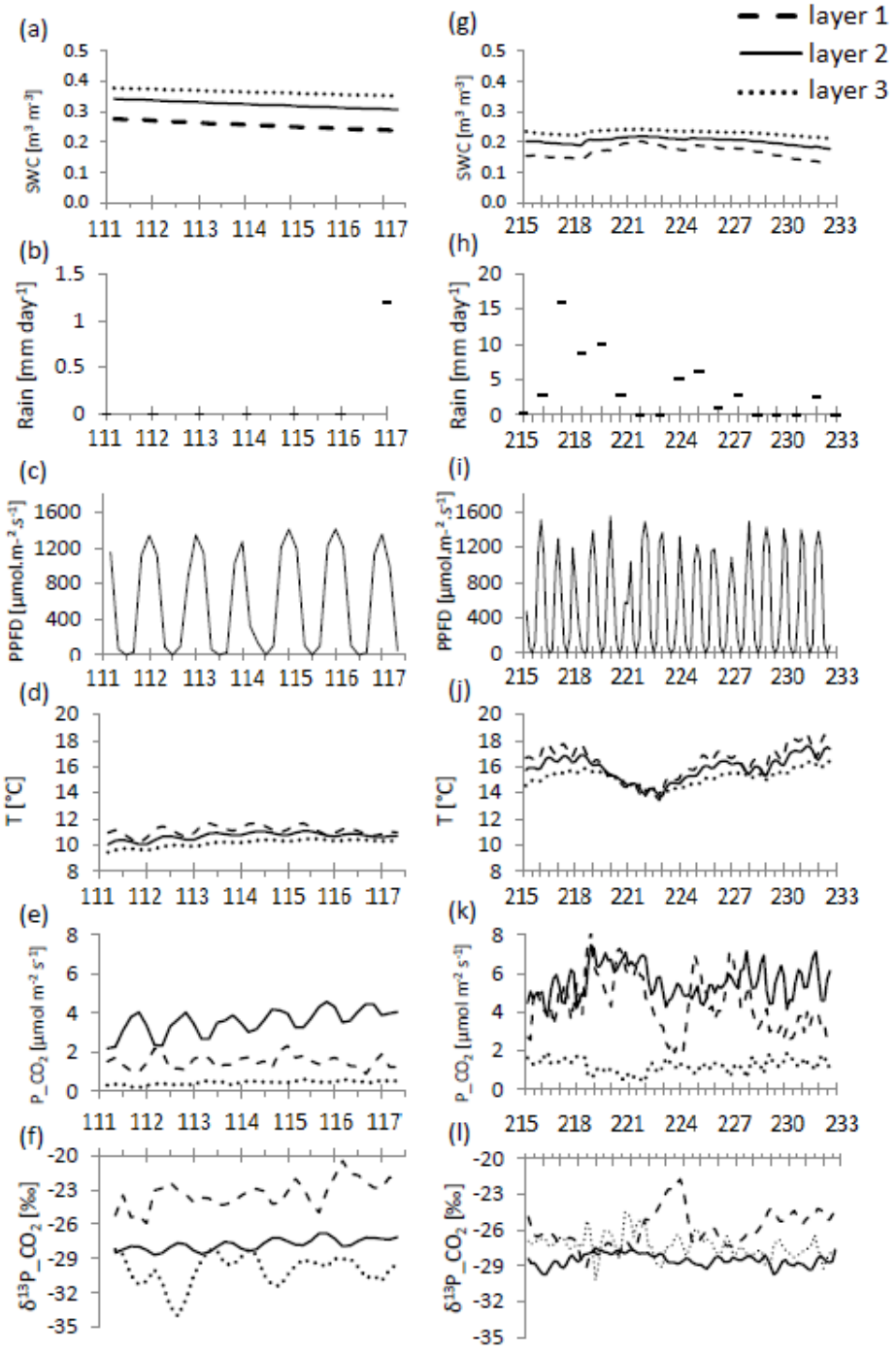

585 **Figure 4: Values over time for soil water content (SWC), rain, photosynthetic photon flux density (PPFD), temperature (T), production (P_CO_2) and its isotopic composition ($\delta^{13}P\_CO_2$) in each soil layer every 30 min in April (21/04 to 27/04, a to f) and in August (03/08 to 21/08, g to l). Dashed line corresponds to layer 1; full line to layer 2 and dotted line to layer 3. T and SCW are measured in the middle of each layer. Longer crosslines on x axes indicate noon for each day.**

Biogeosciences Discuss., doi:10.5194/bg-2016-194, 2016
Manuscript under review for journal Biogeosciences
Published: 17 May 2016

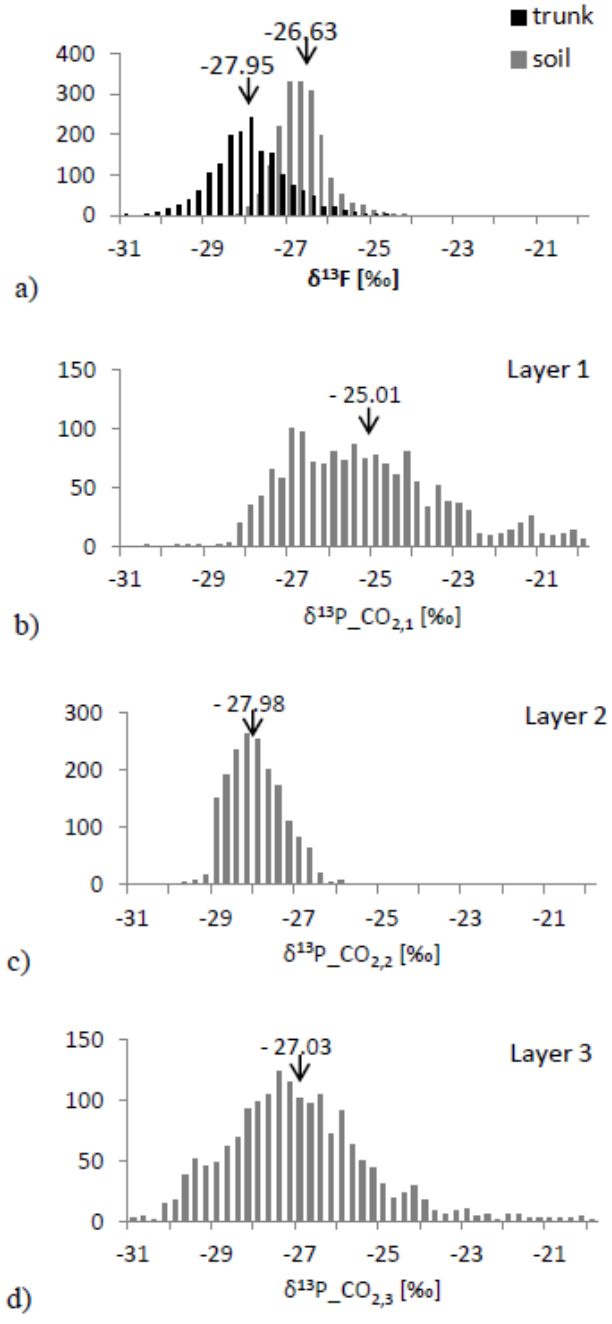

590 **Figure 5: Frequency distribution of the isotopic signature (a) of soil CO_2 efflux ($\delta^{13}F_S$, grey) and trunk CO_2 efflux ($\delta^{13}F_t$, black); and soil CO_2 production ($\delta^{13}P\_CO_2$) every 30 minutes over the four studied periods within each layer for (b) layer 1, (c) layer 2 and (d) layer 3. The average δ^{13} value is indicated with an arrow on each panel.**

Biogeosciences Discuss., doi:10.5194/bg-2016-194, 2016
Manuscript under review for journal Biogeosciences
Published: 17 May 2016

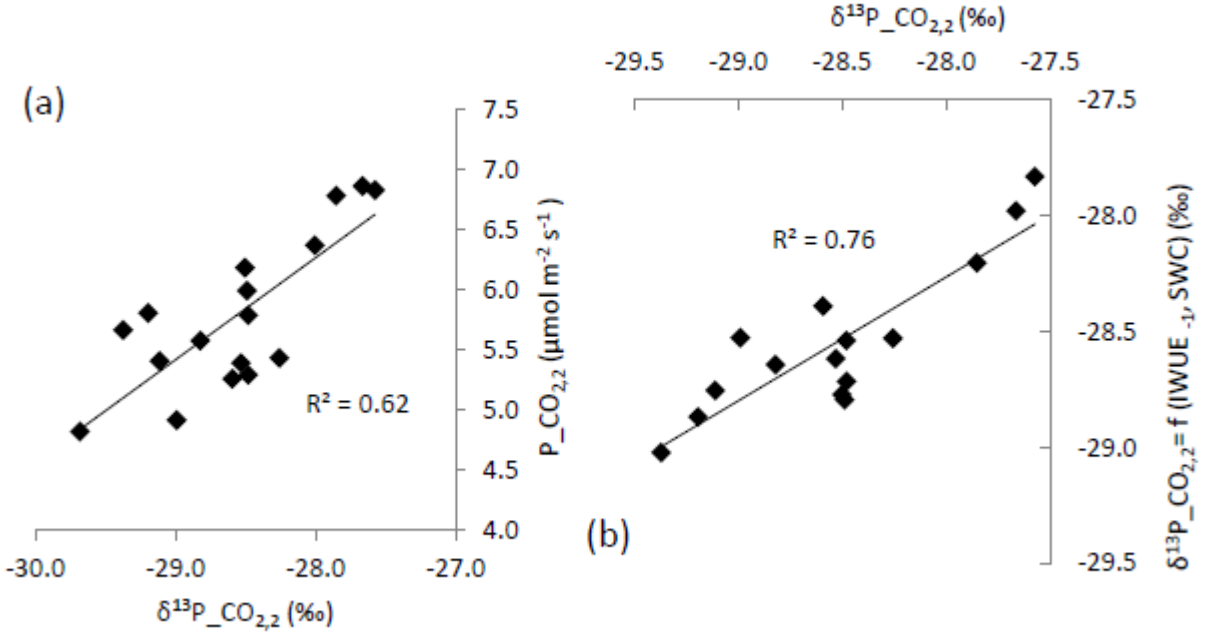

595

Figure 6: Relation (a) between day-to-day variation in daily means of $\delta^{13}P\_CO_{2,2}$ during August (03/08 to 21/08) and day-to-day variation in daily means of $P\_CO_{2,2}$, and (b) between daily means of observed $\delta^{13}P\_CO_{2,2}$ and predicted $\delta^{13}P\_CO_{2,2}$ using a multivariate linear regression against SWC measured at 15 cm on the same day and IWUE measured the previous day.

Biogeosciences Discuss., doi:10.5194/bg-2016-194, 2016
Manuscript under review for journal Biogeosciences
Published: 17 May 2016

600

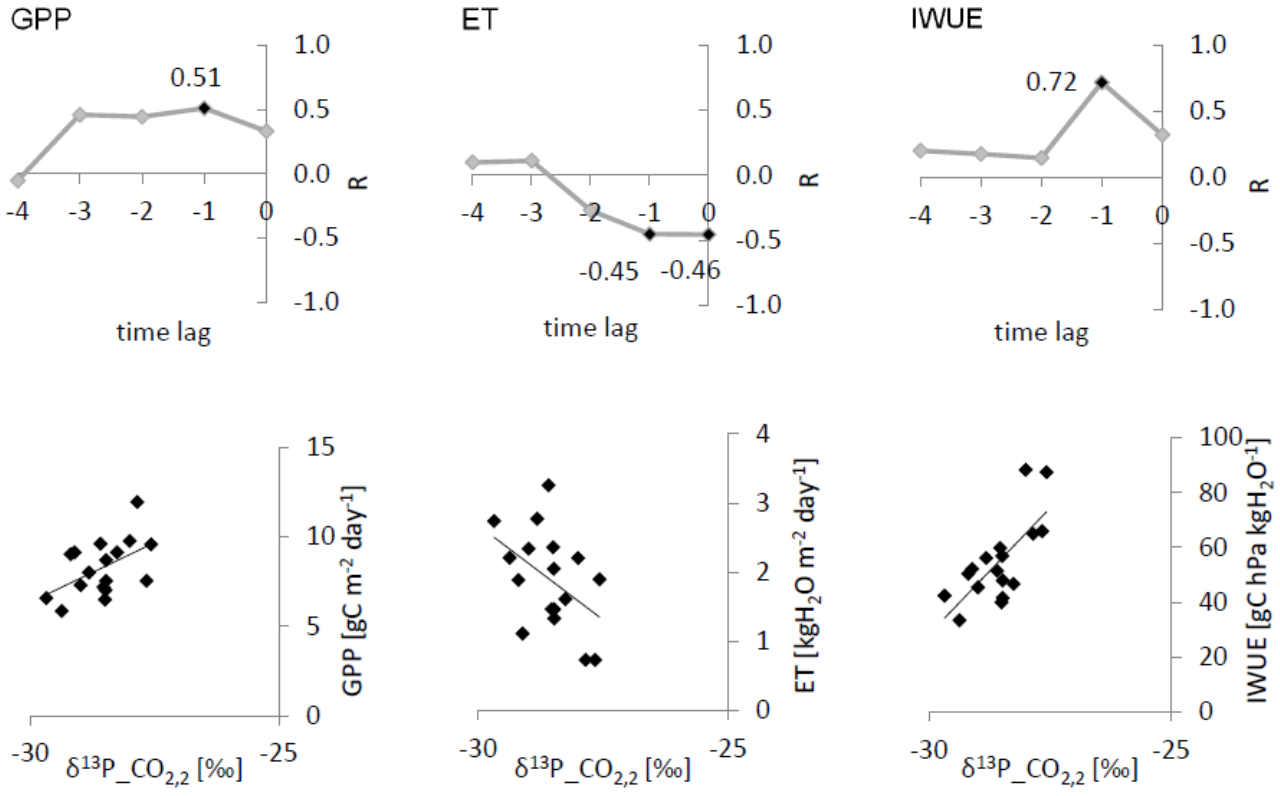

Figure 7: Upper panels: Correlation coefficients between daily means of $\delta^{13}P\_CO_{2,2}$ and gross primary production (GPP, left), evapotranspiration (ET, middle) and inherent canopy water use efficiency (IWUE, right) with a lag ranging from 0 to 4 days. Maximum correlations are identified by black diamonds and the corresponding linear regression is plotted below.

605